Image distortion due to metal sphere in a phantom: comparison of 2D and 3D TSE, and 2D View Angle Tilting

T. A. Hopper[1,2], H. Song[2], J. M. Pope[1], F. W. Wehrli[2]

[1]School of Physical and Chemical Sciences, Queensland University of Technology, Brisbane, Queensland, Australia, [2]Department of Radiology, University of Pennsylvania, Philadelphia, Pennsylvania, United States

Introduction

Magnetic susceptibility differences between materials can cause significant artifacts in MR images [1]. The maximum value of the induced field ΔB is proportional to the difference in susceptibility between the perturber and the tissue and the field shift causes the spins to be spatially mismapped in both frequency-encoding and slice-selection directions. Imaging of patients with metallic prosthetic devices is therefore problematic and a solution of these difficulties would expand MRI's capabilities for evaluating such patients. An application of particular interest is the early detection of mechanical loosening of orthopedic implants and presence of foreign body granulomatosis at the interface of the prosthesis and surrounding medium [2]. The preferred implant material is stainless steel (as opposed to titanium which has more favorable magnetic properties). Typically, the susceptibility of stainless steel is on the order of χ = 3000 to 6000 ppm (S.I). Several approaches have been proposed for alleviating susceptibility-induced artifacts. Among these are increased receive bandwidth, single point mapping (SPI - all phase-encoding) [3] and View Angle Tilting (VAT) [4, 5] The purpose of this study was to investigate the image artifacts resulting from a stainless steel object by comparing 2D and 3D spin-echo pulse sequences at various bandwidths with 2D VAT.

Methods

Using a phantom consisting of a 8mm diameter stainless steel (non-ferromagnetic) sphere centered in a cylindrical tube of agarose gel, MRI was used to observe slice distortion effects caused by the magnetic susceptibility differences between a metallic sphere and gel. 2D and 3D images were obtained using a turbo spin-echo (TSE) sequence and additional 2D images were obtained using a modified spin echo (SE) VAT sequence. In VAT a set of compensation gradients is applied in the slice direction at the same time as the read out gradients and with the same amplitude as the slice select gradients. The VAT method reduces the artifact in the in-plane frequency encoding direction but does not correct for the slice distortion. Axial images were obtained on a Siemens 1.5 T Sonata system using a head coil. Imaging parameters were as follows: TR 500ms, TE 28, 12, 15 (3D, 2D, SE VAT) ms, FOV of 300 mm, matrix size of 256 × 256, 32 slices, 3 mm slice thickness, 3 mm slice separation (2D), and a bandwidth (BW) of 130 and 300 Hz / pixel. The direction of B_0 is into the page and frequency encoding direction is R / L.

Results and Discussion

Fig. 1 shows 2D and 3D TSE images for BWs of 130 and 300 Hz / pixel through the center of the sphere. It is noticed that the bright signal offset to the left in the 2D images, is not present in the corresponding 3D images, indicating the effect of the field perturbation on 2D slice selection whilst the distortion is absent in the 3D phase encoded slice direction. As expected the increased bandwidth reduces the in-plane frequency distortions. Fig. 2 shows 2D VAT at the same slice location. It is noted that the bright intensity artifacts seen in the 2D images of Fig. 1 are absent in the VAT image. Fig. 3 displays images corresponding to a slice location offset by 9 mm from the center of the sphere (i.e. about 5 mm from the edge of the sphere). Both 2D and 3D spin-echo show significant distortions. However, there are significant differences between 2D and 3D. Since slice distortion is absent in 3D, the mean signal in a fixed ROI volume should be similar in all slices outside those that contain the object. This is borne out by a comparison of the mean signal profiles in Fig. 4, showing that for the 3D image a dip occurs at the object boundaries. In contrast, the signal perturbation in the 2D image extends far beyond the object boundaries primarily due to the variations in slice thickness. 2D VAT does not remedy the problem since slice distortion remains.

The positional shift in readout direction caused by a field inhomogeneity of ΔB_Z is $\Delta x = \Delta B_Z(x,y,z) / G_R$, where G_R is the readout gradient. If we consider that the maximum field shift caused by a perturber with susceptibility difference $\Delta\chi$ is $\Delta B_{MAX} = \Delta\chi B_0$, a stainless steel object ($\Delta\chi$~3000 ppm) can produce a field shift of 45 G causing distortions in readout direction up to 10 cm with a read gradient of 4 G/cm! Similarly, in 2D slice-selective imaging such a field shift can cause very large local slice distortions.

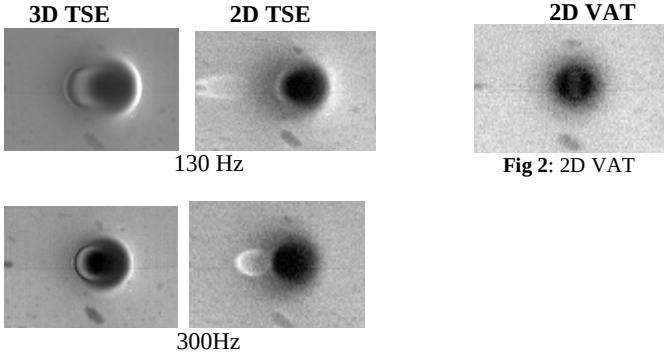

Fig1: 3D and 2D TSE, BW 130 and 300 Hz / Pixel. Located at center of sphere.

Fig 2: 2D VAT

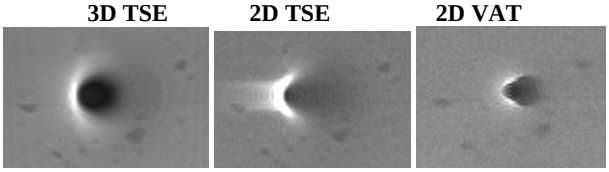

Fig 3: 3D, 2D and 2D VAT at slice location of 9mm from center of sphere and a BW of 130 Hz /pixel

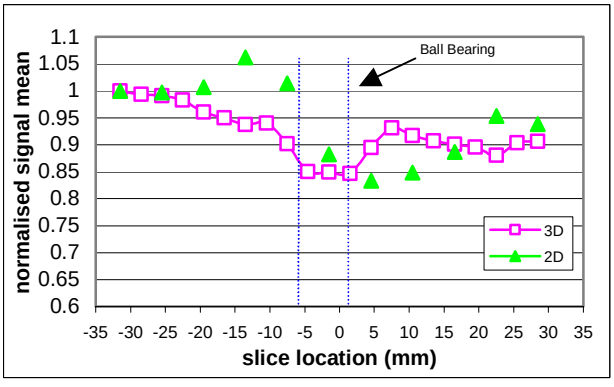

Fig 4: Graph of normalized signal mean vs slice location for 3D and 2D TSE at BW of 300 Hz / pixel. Blue dashed lines indicate boundaries of sphere. The slight drift in the average intensity is likely due to the coil inhomogeneity of receive only phased array head coil.

Conclusion

The very large magnetic field perturbations induced by stainless steel materials cannot currently be remedied with any of the approaches discussed. However, it is obvious that implant materials with susceptibilities lower by one order of magnitude, such as titanium, should be MR compatible with the above techniques.

References

[1] Schenck, J.F., Med Phys, 1996. **23**: p. 815-850.
[2] White, L.M., et al, Radiology, 2000. **215**: p. 254-262.
[3] Balcom, B., et al, JMRI 1996, **123**: p. 131-134.
[4] Cho, Z.H., et al, Med Phys, 1988. **15**: p. 7-11.
[5] Olsen, R.V., et al, Radiographics, 2000. **20**: p. 699-712.